

## EFFECT OF PLATE CURVATURE ON BLAST RESPONSE OF CARBON COMPOSITE PANELS: EXPERIMENTAL INVESTIGATION

Puneet Kumar<sup>1</sup>, David S. Stargel<sup>2</sup>, Arun Shukla<sup>1\*</sup>

<sup>1</sup>Dynamic Photomechanics Laboratory, Department of Mechanical, Industrial and Systems Engineering, University of Rhode Island, Kingston, RI 02881, USA.

<sup>2</sup>Air Force Office of Scientific Research, Aerospace, Chemical, and Material Sciences, 875 N. Randolph Street, Suite 325, Room 3112, Arlington VA, 22203-1768

\*Corresponding author email: shuklaa@egr.uri.edu

**Keywords:** Carbon fiber, Shock loading, Dynamic response, DIC.

### Abstract

*Experimental studies were conducted to understand the effect of plate curvature on the blast response of 32 layered carbon fiber panels. A shock tube apparatus was utilized to impart controlled shock loading on carbon fiber panels having three different radii of curvatures; infinity (panel A), 304.8 mm (panel B), and 111.76 mm (panel C). Panels with dimensions of 203.2 mm x 203.2 mm x 2 mm were held with clamped boundary conditions during the shock loading. A 3D Digital Image Correlation (DIC) technique coupled with high speed photography was used to obtain out-of-plane deflection and velocity, as well as in-plane strain on the back face of the panels. Panel A and panel B had mid-point deflections of 14 mm and 18 mm, respectively, before failure initiated. The mid-point deflection was 10 mm in panel C prior to catastrophic failure. Macroscopic postmortem analysis was also performed on all the panels to comprehend and compare the different mechanisms of failure observed in the three panels. Basically, there are two types of failure mechanisms observed in all the three panels: fiber breakage and inter-layer delamination. The fiber breakage was induced from the face exposed to shock loading and continued inside. The delamination was visible on the side of the specimen as well as on the face exposed to the shock loading. Macroscopic postmortem analysis and DIC results showed that panel C can mitigate higher intensity (pressure) shock waves without initiation of catastrophic damage in the panel. Panel B could sustain the least shock wave intensity and had catastrophic failure (panel disintegrating into small pieces). Panel A could mitigate the blast pressure having intensity in between the intensities impinging on the other two panels.*

## 1 Introduction

A controlled experimental study has been conducted to understand the effect of plate curvature on the blast response of carbon composite panels. Accidental explosions or bomb blasts cause extreme loading on structures, which have both flat and curved geometries (as in the USS Cole [1] and Oklahoma State [2] bombing). Therefore it is important to understand the effect of curvature on the blast response. Also, a better understanding of the effect of curvature will help in manufacturing new structures with better blast resistant property. Carbon composite panels having three different radii of curvature were subjected to shock loading using a shock tube in order to study their dynamic response. The choice of these panels was motivated by the study on the ballistic response of these panels by Stargel [3]. Real-time and post-mortem analysis was conducted on the panels to evaluate the effects of plate curvature on blast mitigation. In particular, the midpoint transient deflection, velocity, and macroscopic post-mortem analysis of the panels has been used to characterize the response of curved panels when subjected to a controlled blast loading.

There is a large volume of literature dealing with the blast loading of structures [4-13]. For brevity of space, only a few studies are mentioned here. Franz *et al.* [14] studied the response of glassfiber chopped-strand mat laminates to air pressure blast. They found matrix cracking, delamination/debonding, and penetration as final damage in monolithic and layered laminates with varying areal density. Ochola *et al.* [15] concentrated on strain rate sensitivity of both carbon fiber reinforced polymer and glass fiber reinforced polymer by testing a single laminate configuration with strain rate varying from  $10^{-3}$  and  $450 \text{ s}^{-1}$ . Results showed that the dynamic material strength for GFRP increases with increasing strain rate and the strain to failure for both CFRP and GFRP decreased with increasing strain rate. LeBlanc and Shukla [16] studied the underwater shock loading response of E-glass/Vinyl ester curved composite panels. They used the 3D-DIC system for measuring the transient response during the experiments. They also compared the experimental results to simulation results obtained from the commercially available Ls-Dyna finite element code, which showed a high level of correlation using the Russell error measure. Shen *et al.* [17] experimentally investigated the response of sandwich panels with aluminum face sheets and aluminum foam core. Panels with varying curvatures (two different curvatures), and different core/face sheet configurations were tested at three different blast intensities. They found that the initial curvature of the sandwich panel changes the deformation mode and improved the performance of the structure when compared to equivalent flat plate.

The present study was performed using carbon fiber composite panels having three different curvatures. The results from this study show that the plate curvature affects the blast mitigation property. As the radius of curvature decreases (becomes more sharply curved), the response of panels to sustain shock loading changes.

## 2. Experimental Procedure

### 2.1 Specimen Geometry and Material Details

Panels with three different radii of curvature were utilized in the experiments: infinite radius of curvature (Panel A), 304.8 mm radius of curvature (Panel B) and 111.8 mm radius of curvature (Panel C). The specimens are shown in fig. 1. The specimens were fabricated using ready-to-cure sheets of unidirectional AS4/3501-6 material manufactured by the Hercules Corporation of

Magna, Utah. These sheets were manufactured by pulling a row of uniformly spaced fibers through resin bath. The spacing between the fibers determines the ratio of fiber volume to total volume of the material. After stacking 32 plies of these unidirectional material in the desired orientation, the panels were vacuum bagged and then placed in autoclave for curing. The curved panels were manufactured in the same way as described above with a difference that cylindrically curved pre-forms were used for laminate lay-up and curing. The orientation of the individual unidirectional plies that comprised the composite laminate was selected to simulate quasi-isotropic properties  $([0/90/+45/-45]_{4s})$ . Each experiment was repeated three times to assure consistent results. The specimens were 203 mm long x 203 mm wide x 2 mm thick, made out of 32 layers of carbon fibers. For the case of curved panels, the arc length of the curved edges corresponds to the plate length.

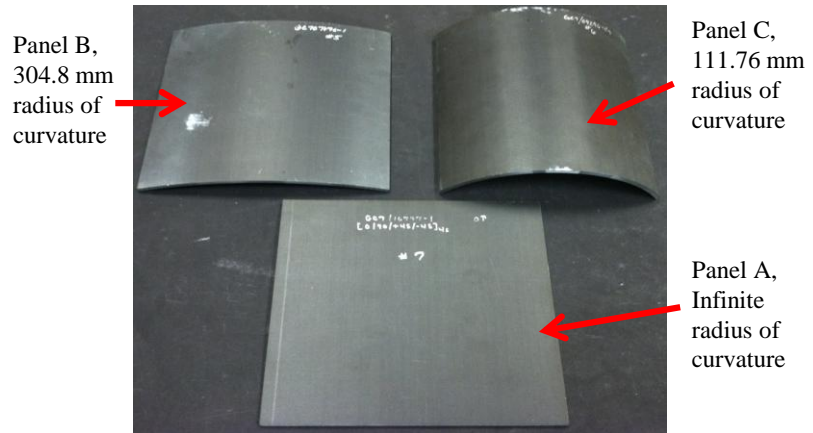


Figure 1. Specimen Geometries

## 2.2 Shock loading apparatus and loading conditions

The shock tube apparatus used in this study to obtain the controlled dynamic loading is shown in fig. 2. A complete description of the shock tube and its calibration can be found in [19]. The shock tube consists of a long rigid cylinder, divided into a high-pressure driver section and a low pressure driven section, which are separated by a diaphragm. By pressurizing the high-pressure section a pressure difference across the diaphragm is created. When this pressure differential reaches a critical value, the diaphragm ruptures. The subsequent rapid release of gas



Figure 2. URI shock tube facility

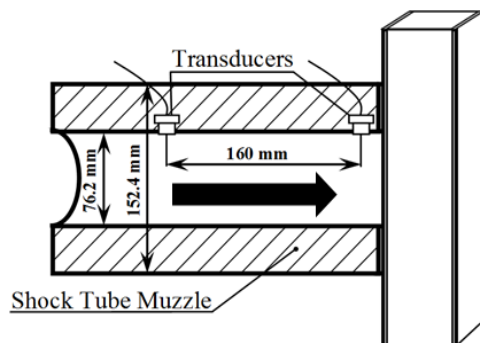


Figure 3. Shock tube muzzle

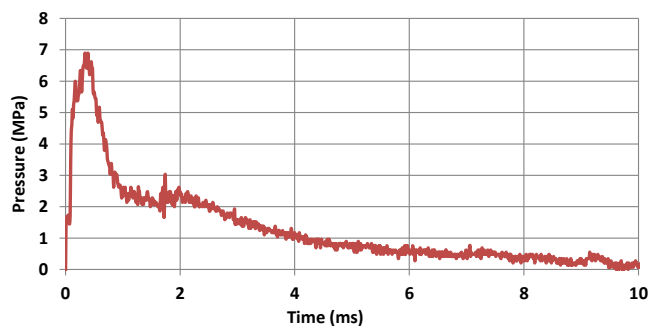


Figure 4. Typical Pressure profile

creates a shock wave, which travels down the shock tube to impart shock loading on the specimen at the muzzle end.

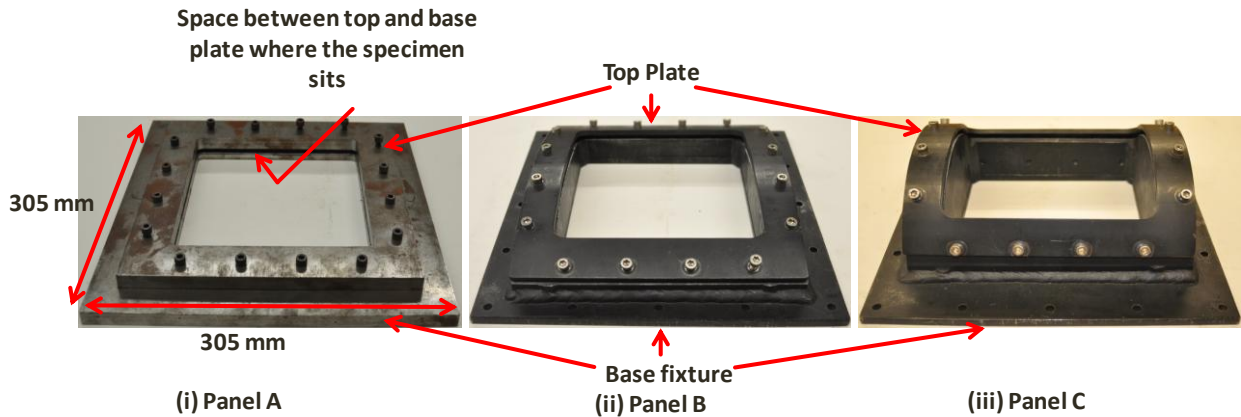


Figure 5. Loading Fixture

The shock tube utilized in the present study has an overall length of 8 m, consisting of driver, driven, converging and muzzle sections. The diameter of the driver and driven section is 0.15 m. The final muzzle diameter is 0.07 m. Two pressure transducers (fig. 3), mounted at the end of the muzzle section measure the incident shock pressure and the reflected shock pressure during the experiment. The incident shock wave pressure was kept constant for all of the experiments. A typical pressure profile obtained at the transducer location closer to the specimen is shown in fig. 4. The specimens were shock loaded at three different pressures varying from 3 MPa to 8 MPa. At each of the three pressures, experiments were repeated three times to validate the consistency. The specimens were held with clamped boundary conditions on all the four edges. Appropriate fixtures for holding each of the plate geometries are shown in fig. 5.

### 3. Experimental results and Discussion

#### 3.1 DIC Analysis

The DIC technique is used to obtain the out-of-plane deflections and velocities as well as the in-plane strains on the back surface for all the three geometries. The shock tube used in this study provides a uniform pressure pulse over a circular area of 4562 mm<sup>2</sup> (muzzle area). This is verified by the DIC image of the out of plane displacement on flat plate during shock impingement as shown in fig. 6. The image taken at 50 μs shows that the flat panel had a uniform deflection of 3 mm ± 0.2 mm within a central region of diameter 72 mm. As the muzzle diameter of the shock tube is 76 mm, the uniform deflection contour constitutes about 92% of the total loaded area. This out of plane deflection decays to 0 mm from 3 mm in an area of thickness 3 mm beyond this central region.

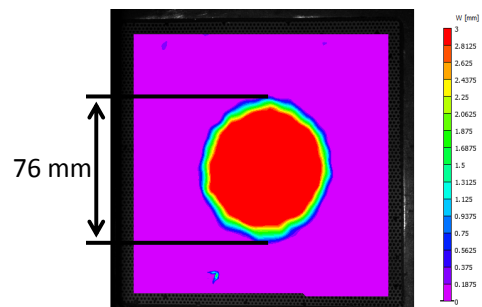


Figure 6. Out of plane deflection at  $t = 50 \mu s$

The full-field deflection at the failure loading for the panels is shown in fig. 7. The total deflection in these panels subjected to blast loading comprises of two distinct regions, namely, the indentation region followed by the flexural deflection (fig. 8). During indentation, localized deflection superpose onto the overall deflection. In case of flexure, the overall deflection starts to overpass the localized deflection. The indentation deflection is localized around the loading area whereas a full field deflection over the area of the specimen being loaded is predominant in flexural mode. Also, the boundary conditions affect the deflection in case of flexural mode. Panels B and C had elliptical deflection contour at 200  $\mu$ s. Since both these panels are curved, the shock wave impinges on the projected area and creates localized elliptical deflection contour. Panel B had fluid-structure interaction for first 200  $\mu$ s at which time the boundary condition starts affecting the deflection development. Around 200  $\mu$ s, the elliptical deflection contour in panel B starts changing to rectangular shape because of the boundary conditions. Also, the deflection mode in panel B changes from indentation to flexural mode at this time. The deflection in panel C continues to develop further with elliptical contour. The deflection is primarily because of indentation and boundary conditions do not affect the deflection contours. As such, it retains its elliptical shape throughout the loading process.

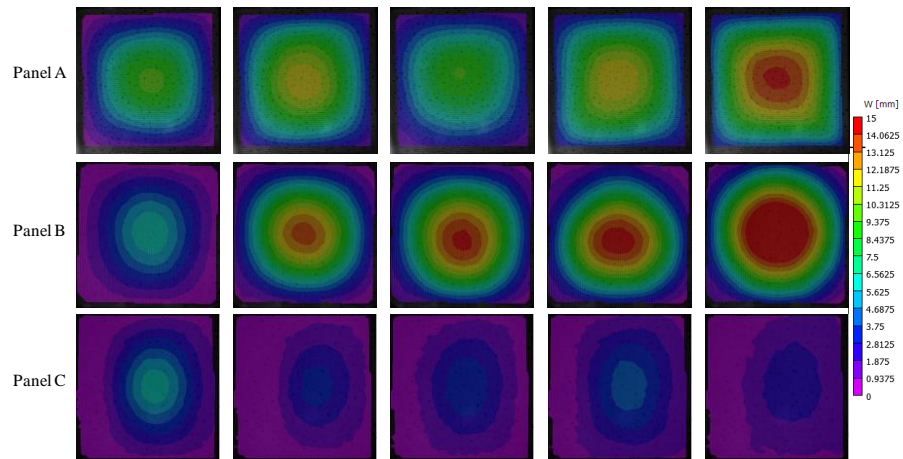


Figure 7. Full field deflection of panels from 3D-DIC analysis

Also, the boundary conditions affect the deflection in case of flexural mode. Panels B and C had elliptical deflection contour at 200  $\mu$ s. Since both these panels are curved, the shock wave impinges on the projected area and creates localized elliptical deflection contour. Panel B had fluid-structure interaction for first 200  $\mu$ s at which time the boundary condition starts affecting the deflection development. Around 200  $\mu$ s, the elliptical deflection contour in panel B starts changing to rectangular shape because of the boundary conditions. Also, the deflection mode in panel B changes from indentation to flexural mode at this time. The deflection in panel C continues to develop further with elliptical contour. The deflection is primarily because of indentation and boundary conditions do not affect the deflection contours. As such, it retains its elliptical shape throughout the loading process.

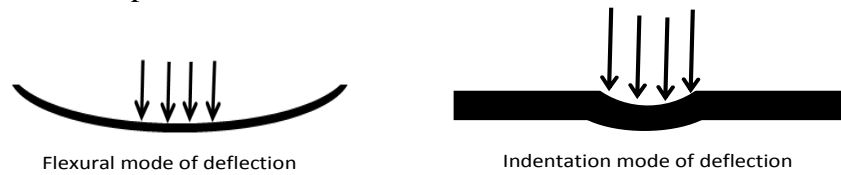


Figure 8. Deformation mechanism observed in panels

Also, the deflection mode in panel B changes from indentation to flexural mode at this time. The deflection in panel C continues to develop further with elliptical contour. The deflection is primarily because of indentation and boundary conditions do not affect the deflection contours. As such, it retains its elliptical shape throughout the loading process.

### 3.2 Energy analysis

For a better understanding of the energy mitigating behavior of the panels, the incident energies need to be same. Thus, the energy distribution analysis for all the three panels was also performed at same loading pressure. The incident energy was nearly same in all the three panels. The three panels had different amount of

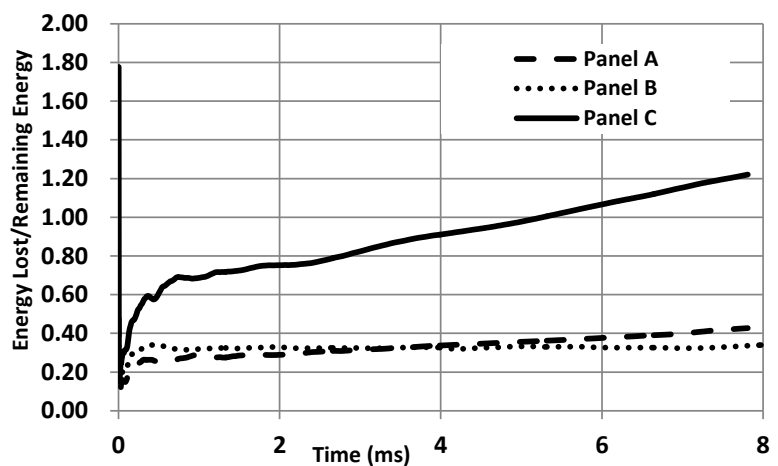


Figure 9. Ratio of energy lost to remaining energy for the three panels at failure loading.



energy dissipation which depended on the individual blast mitigation property of the respective curvature. Panel C had the maximum energy lost whereas panel B had the least energy lost. To better understand the energy dissipation behavior of the panels, the ratio of energy lost to the remaining energy was calculated and is shown in fig. 9. Panel C had the best energy mitigation as the ratio of energy lost to the remaining energy is maximum. The curvature of panel C causes the impinging energy on it to dissipate along its curved surface and improve the blast mitigation of the panel.

### 3.3 Macroscopic post-mortem analysis

The post-mortem image of the shock loaded flat carbon composite panel A (at failure loading) is shown in fig. 10. There is inter-layer delamination and fiber breakage evident in the post-mortem analysis. The fiber breakage initiated from the clamping edges. To better understand the failure, the panel was divided into three regions and a close postmortem analysis was done on each of the regions. The close-up postmortem images of region 1 (fig. 10) shows that there is fiber breakage in multiple layers. The fiber breakage continues up to 7 layers from the side which was subjected to shock loading. Carbon composite panels are brittle. When they are subjected to shock loading, there is deflection in the panel, but the clamping tries to restrain this deflection. This restrain from the clamping causes the fiber breakage initiation. There is fiber breakage and delamination which extends to the third layer, is visible in region 2. As seen in the macroscopic postmortem image of region 2, there is transverse fiber breakage. The delamination and fiber breakage in region 2 also started from the clamping boundary as in the region 1. There is fiber breakage and delamination in region 3 around the clamping boundary. At the same time there is fiber breakage and delamination on the edge of the panel as seen in the macroscopic post-mortem image of region 3. Again, to brevity of space the post-mortem analysis for panel B and panel C will be presented during the conference.

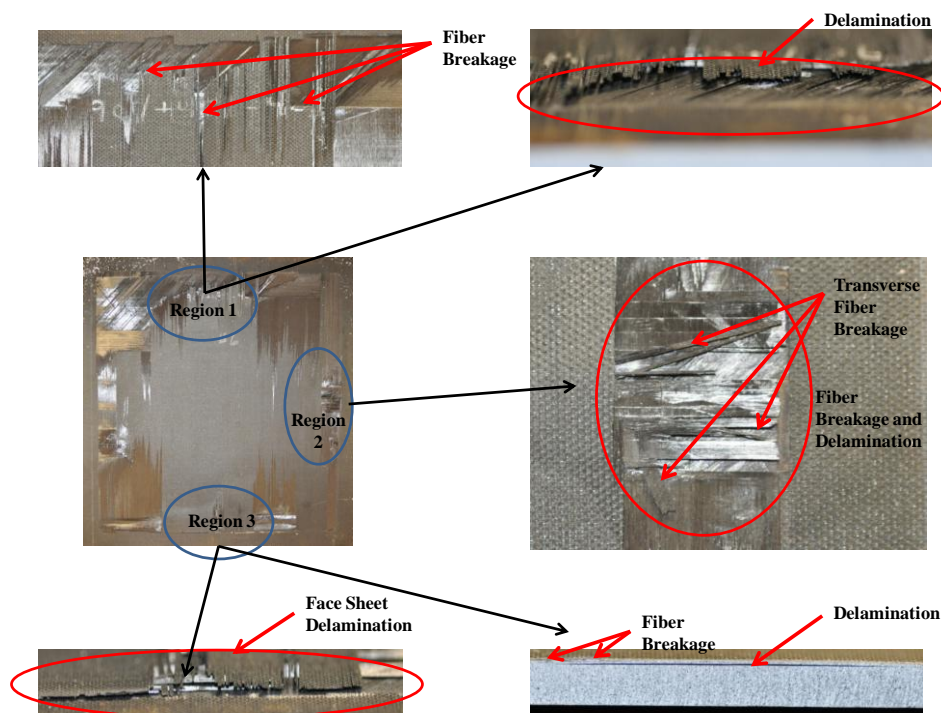


Figure 10. Post-mortem image of Panel A

#### **4. Conclusions**

Three types of panels with varying curvature have been subjected to a controlled shock loading using a shock tube. 3D DIC technique coupled with high speed photography is used to obtain the out-of-plane deformation/velocity and in-plane strain on the back face of all the three panels.

1. The macroscopic post-mortem analysis and DIC deflection, velocity and in-plane strain analysis shows that panel C (112 mm radius of curvature) is capable of sustaining the highest threshold failure load.
2. The flexural deformation decreases and indentation deformation increases as the radius of curvature decreases. There is a limit to which the radius of curvature can be decreased. As the radius of curvature reduces to a limiting value, the shock wave will glide over the surface.
3. The energy analysis showed that the Panel C (having least radius of curvature) had a higher ratio of lost energy to the remaining energy. This shows that panel C had the best energy dissipation property as compared to the other two curvatures.

#### **5. Acknowledgement**

The authors acknowledge the financial support provided by the Department of Homeland Security (DHS) under Cooperative Agreement No. 2008-ST-061-ED0002. The financial support provided by the Office of Naval Research under Grant No. N00014-10-1-0662 (Dr. Y.D.S. Rajapakse) is also acknowledged.

#### **References**

- [1] R. Perl, and R. O'Rourke, Terrorist Attack on USS Cole: Background and Issues for Congress, CRS Report for Congress, 2001.
- [2] The Oklahoma City Bombing: Improving Building Performance through Multi-Hazard Mitigation, Federal Emergency Management Agency Mitigation Directorate, FEMA 277, August 1996.
- [3] D.S. Stargel, Experimental and Numerical Investigation into the effects of Panel Curvature on the High Velocity Ballistic Impact Response of Aluminum and Composite Panels, Doctor of Philosophy Dissertation, University of Maryland, College Park, 2005.
- [4] L. Chun, and K.Y. Lam, Dynamic analysis of clamped laminated curved panels, *Compos. Struct.*, 30 (1995) 389-398.
- [5] R. Rajendran, and J.M. Lee, Blast loaded plates, *Mar. struct.*, 22 (2009) 99-127.
- [6] S.A. Tekalur, K. Shivakumar, and A. Shukla, Mechanical behavior and damage evolution in E-glass vinyl ester and carbon composites subjected to static and blast loads, *Composites: Part B*. 39 (2008) 57-65.
- [7] H. Arora, P.A. Hooper, and J.P. Dear, Dynamic response of full-scale sandwich composite structure subject to air-blast loading, *Composites: Part A*, 42(2011) 1651-1662.
- [8] P. Kumar, J. LeBlanc, D. S. Stargel, A. Shukla, Effect of plate curvature on blast response of aluminum panels, *International Journal of Impact Engineering*, 46 (2012) 74-85.
- [9] T. Franz, G.N. Nurick, M.J. Perry, Experimental investigation into the response of chopped strand mat glassfibre laminates to blast loading, *International Journal of Impact Engineering*, 27(2002) 639-667.
- [10] R.O. Ochola, K. Marcus, G.N. Nurick and T. Franz, Mechanical behavior of glass and carbon fiber reinforced composites at varying strain rates, *Composites Structures*, 63(2004) 455-467.
- [11] J. LeBlanc, and A. Shukla, Dynamic response of curved composite panels to underwater explosive loading: experimental and computational comparisons, *Compos. Struct.*, 93 (2011) 3072-3081.

- [12] J. Shen, G. Lu, Z. Wang, L. Zhao, Experiments on curved sandwich panels under blast loading, *International Journal of Impact Engineering*, 37(2010) 960-970.
- [13] T. Hause, and L. Librescu, Dynamic response of doubly-curved anisotropic sandwich panels impacted by blast loadings, *International Journal of Solids and Structures*, 44(2007) 6678-6700.
- [14] M. M. Shokrieh, and L. B. Lessard, Progressive Fatigue damage Modelling of Composite Materials, Part II: Material Charecterization and Model Verification, *Journal of Composite Materials*, 34 (2000) 1081-1116.
- [15] J. LeBlanc, A. Shukla, C. Rousseau, and A. Bogdanovich, Shock loading of three-dimensional woven composite materials, *Compos. Struct.*, 79 (2007) 344–355.
- [16] J. Wright, *Shock Tubes*, John Wiley and Sons Inc., New York, 1961.
- [17] E. Wang, and A. Shukla, Analytical and experimental evaluation of energies during shock wave loading, *International Journal of Impact Engineering*, 37 (2010), 1188-1196.
- [18] V. Tiwari, M.A. Sutton, S.R. McNeill, S. Xu, X. Deng, W.L. Fourney, and D. Bretall, Application of 3D image correlation for full-field transient plate deformation measurements during blast loading, *Int. J. Impact Eng.*, 36 (2009) 862-874.
- [19] N. Gardner, E. Wang, P. Kumar, and A. Shukla, Blast Mitigation in a Sandwich Composite Using Graded Core and Polyurea Interlayer, *Exp. Mech.*, DOI 10.1007/s11340-011-9517-9 (2011).